Taylor & Francis
Taylor & Francis Group

SEPARATION SCIENCE AND TECHNOLOGY

Separation Science and Technology

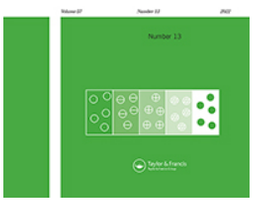

ISSN: 0149-6395 (Print) 1520-5754 (Online) Journal homepage: www.tandfonline.com/journals/lsst20

A novel carbon-based material recycled from end-of-life tires (ELTs) for separation of organic dyes to understand kinetic and isotherm behavior

Ilknur Özüdoğru, Zehra Yigit Avdan & Senay Balbay

To cite this article: Ilknur Özüdoğru, Zehra Yigit Avdan & Senay Balbay (2022) A novel carbon-based material recycled from end-of-life tires (ELTs) for separation of organic dyes to understand kinetic and isotherm behavior, Separation Science and Technology, 57:13, 2024-2040, DOI: 10.1080/01496395.2022.2029489

To link to this article: https://doi.org/10.1080/01496395.2022.2029489

SEPARATION SCIENCE AND TECHNOLOGY
2022, VOL. 57, NO. 13, 2024–2040
https://doi.org/10.1080/01496395.2022.2029489

Taylor & Francis
Taylor & Francis Group

A novel carbon-based material recycled from end-of-life tires (ELTs) for separation of organic dyes to understand kinetic and isotherm behavior

Ilknur Özüdoğru[a], Zehra Yigit Avdan[a], and Senay Balbay[b]

[a]Department of Environmental Engineering, Eskisehir Technical University, Eskisehir, Turkey; [b]Department of Waste Management, Vocational School, Bilecik Seyh Edebali University, Bilecik, Turkey

ABSTRACT

Within the scope of end-of-life tires (ELTs) management, recovery of tires considering circular economy approach is becoming increasingly important. This study aims to examine the sorptive behavior of methylene blue (MB) and Rhodamine B (RB) dyes from synthetic textile industry discharge with a carbon-based sorbent (CBM) recycled from ELTs as a novel patented method and used for the first time for organic dye removal in the literature. The CBM was characterized by using fourier transform infrared (FTIR) and scanning electron microscopy (SEM) for structural and morphological properties. XRD (X-ray diffraction) and XPS (X-ray photoelectron spectroscopy) analysis were used for phase composition and surface chemistry of CBM. The maximum adsorption capacity of MB and RB on CBM is 681.14 and 85.26 mg/g, respectively. For the reusability of the CBM, the regeneration experiment was carried out and MB and RB removal performance of CBM gradually decreased with increasing adsorption cycles. The results show that it is possible to utilize CBM which in terms of ensuring the reuse of wastes within the scope of industrial symbiosis, as an effective adsorbent in dye removal. This study reduces environmental pollution by converting the end-of-life tires into carbon-based material for water/wastewater treatment provides a "win-win" solution to improve waste management.

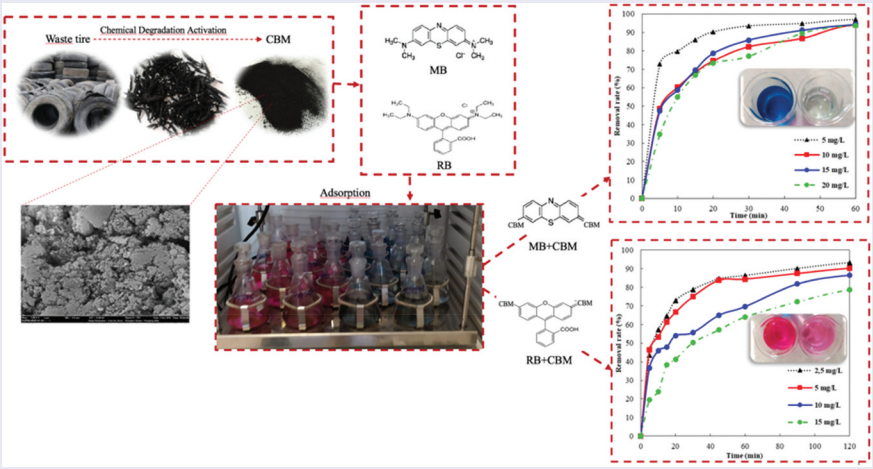

ARTICLE HISTORY
Received 25 September 2021
Accepted 10 January 2022

KEYWORDS
Waste tires; carbon-based material; methylene blue; Rhodamine B; material recycling; reusability; circular economy

INTRODUCTION

Environmental pollution is one of the enormous problems encountered today with increasing industrial activities every year; it causes severe problems for Earth. Currently, dyes are widely used in many areas such as rubber, paper, leather, plastic, cosmetics, medicine, pigment production, printing, food and drink, photoelectrochemical cell, chemical, and petrochemical industry, notably in the textile industry.[1–10] Such industries generate significantly high amounts of wastewater contaminated with organic dyes[11] and situations leading to water pollution due to uncontrolled wastewater discharges.[3] Most dyes are chemically and thermally stable and also non-biodegradable. In addition, dyes constitute the major problem, such as toxic effects on the environment, humans, aquatic creatures, and bioaccumulation in nature.[8,11–16] Dyes also slow down the

CONTACT Zehra Yigit Avdan zyigit@eskisehir.edu.tr Department of Enviromental Engineering, Eskisehir Technical University, Iki Eylul Campus, Muttalip, Tepebasi, Eskisehir 26555 Turkey
Supplemental data for this article can be accessed on the publisher's website.

photosynthesis of the aquatic environment by preventing the passage of solar radiation and reduce the dissolved oxygen level to cause turbidity in the water environment.[17,18]

Consequently, the ecological balance is deteriorating, and it also causes esthetic problems. Dyes must be treated before discharging because of such environmental issues.[19,20] Physical, chemical, and biological treatment methods have been used for dye removal.[2,3,5] Of these methods, adsorption is a simple design, wide applicability, easy to use, efficient, effective, and cheap option for dye removal.[21,22] As an adsorbent material, studies on carbon-based adsorbent materials with low energy needs, low cost, and high adsorption capacity have received significant attention from the past and are continuing.[22–24] Concurrently, it is thought that these carbon-based materials will play an active role in dye removal. Exclusively, polymeric wastes such as plastic, rubber, and agricultural wastes are used for low-cost carbon-based material (CBM) production with the conjointly of pyrolysis and carbonization processes. Santoso et al. divided carbon adsorbent materials into six classes as activated carbon, biochar, modified biochar and modified activated carbon, graphitic carbon, and its modification, porous carbon materials, carbon nanotube materials.[22] Among these, activated carbon is widely used for the removal of dyes from wastewater. However, the cost of activated carbon and the existence of problems related to regeneration made it necessary to investigate alternative adsorbents. In this context, waste or end-of-life tires, 80% of which cannot be utilized globally, appear as alternative adsorbents. It is estimated that annual tire production in the world is about 1.5 billion, which means an estimated 17 million tons of used tires.[18,25] The immediate release of end-of-life tires to the environment poses a severe problem for the environment and human health, especially with the chemical spills spreading to the receiving medium and the risk of fire it carries.[26–28] Recycling, recovery, and reuse is the best way to process end-of-life tires in an environmentally friendly treatment.[26] Numerous techniques such as mechanical, thermomechanical, cryomechanical, pyrolysis, chemical degradation, devulcanization, and microbial desulphurization techniques have been proposed to recover end-of-life tires.[29] Balbay and Açıkgöz obtained a novel CBM material which is a unique process they patented different from pyrolysis CBM using end-of-life tires.[29,30] This novel CBM material has been used in different fields as a substitute for carbon black in tire production,[31] as an additive in epoxy,[32] as a carbon source in carbon foam production and for energy storage.[33]

This study aims to determine its usability as an adsorbent for the removal potentials of dyes by using carbon-based material obtained as a result of chemical degradation of end-of-life tires, which creates an environmental issue in the world. The adsorption capacity of this novel carbon-based material as an adsorbent material will be studied for the first time in the literature. Therefore, revealing the adsorption potential on Methylene Blue (MB) and Rhodamine B (RB) using CBM constitutes the unique aspect of the study.

Material and method

Materials and reagents

In this study, two dyes were studied: Methylene Blue (MB, ChemBio, $C_{16}H_{18}ClN_3S{\cdot}xH_2O$, 319.85 g/mol CAS: 122965–43-9) and Rhodamine B (RB, Sigma- Aldrich, $C_{28}H_{31}ClN_2O_3$, 479.01 g/mol, CAS: 81–88-9). These cationic dyes have been chosen because they are found in the wastewater of industries with very intensive production such as textiles and have dangerous and carcinogenic effects on human health.[22,34–36] Sodium hydroxide (NaOH, %97, Merck B920862 648, 40.00 g/mol) and hydrochloric acid (HCl, %37, Merck 1.00314.2500) were used for pH adjustment (0.1 M HCl, 0.1 M NaOH) of dyes in the study. Ultrapure water (Millipore Milli-Q® Direct 8 Water Purification System) was used for all solutions prepared during the experiments.

Carbon-based material (CBM) recycled from end-of-life tires was used as an adsorbent. Balbay and Açıkgöz obtained a unique CBM material, a novel process they patented different from pyrolysis CBM using end-of-life tires.[29,30]

Instrumentation

The pH meter (Thermo Orion Star A321 Portable pH Meter) for adjustment of prepared dyes, UV-Visible spectrophotometer (HACH LANGE DR5000) for scan the wave dye of methylene blue and Rhodamine B solution and to read the absorbance values for the dye concentrations of the samples taken during the experiments, precision scales (OHAUS Adventurer-Pro) for weighing during the experiment and 0.45 µm membrane filter were used for filtration of the dyes samples. All adsorption isotherm and kinetics studies were performed on the WTW TR-1 Heidolph UNIMAX 2010 mixing device.

The morphological and functional group analyses of CBM and adsorbed CBM were characterized by a scanning electron microscope (SEM-ZEISS Supra 40VP) and Fourier transform infrared spectroscopy from 400 to 4000 cm^{-1} (FT-IR; PerkinElmer, model spectrum 100), respectively. For the CBM elemental analysis, a CHNS-628 (LECO) analyzer was used, and ASTM D-5865 method was used for calorific value analysis. Surface area measurement Brunauer-Emmett-Teller (BET) analysis was performed with Micromeritics ASAP 2020 device. Phase composition was determined by XRD (Panalytical Empyrean model high temperature X-ray diffractometry (HT-XRD)) analysis. Data were collected at 2θ from 10◦ to 100◦.[29] Surface chemistry of CBM was determined by XPS spectral analysis. XPS spectral analysis was obtained using X-ray photoelectron spectroscopy (XPS, PHI) using Al monochromatic X-ray anode source for surface chemistry of CBM.

Experimental setup

Batch adsorption experiments of MB and RB were carried out to investigate the adsorption performance of CBM. The experiments were carried out in a mixing device with 50 ml fixed volume MB and RB dyes solutions by adding certain amounts of CBM into 100 ml flasks. There is also a unit to set the temperature where the mixing device is located. Stock dyes solutions were prepared for adsorption experiments, and it has been used in experiments by dilution. Before the analysis, wavelength scanning (Fig. 1) at different concentrations was performed for MB and RB in the UV-Visible spectrophotometer. As seen in Fig. 1, the maximum absorbance value for MB and RB is 664 nm and 554 nm, respectively.

A standard calibration curve (MB; 1–20 mg/L, RB; 1–10 mg/L) was prepared for each dye at these wavelengths where the maximum peak was observed. When the wavelength scans with concentrations higher than 50 mg/L for MB and 15 mg/L for RB, it is seen that there are shifts in the maximum peaks. For this reason, while working at the concentrations where shifts occur, dilution was done, and readings were done in the calibration curve range. The samples taken at certain time intervals during the experiment were filtered through a 0.45 μm membrane filter to analyze the dye concentrations. The readings were done in the UV-Visible spectrophotometer, and the dye solution concentrations were calculated with the help of the calibration curve prepared.

Batch experiments were performed to examine the effect of adsorbent dose (MB; 0.1–0.5 g/L and RB; 0.1–0.75 g/L), pH (MB; pH_0 = 3,4,6,8,10 and RB; pH_0 = 3,4,5,7,9), initial dye concentration (MB; C_0 = 5–10-15-20 mg/L and RB; C_0 = 2.5-5-10-15 mg/L), agitation speed (MB and RB; 100 rpm, 150 rpm, 200 rpm), temperature (MB and RB; 293 K, 303 K, 313 K) and contact time (MB; 0–120 min and RB; 0–210 min) of MB and RB adsorption on CBM. Optimum conditions were determined by these experiments. An adsorption kinetic study was carried out with these data. The dye removal rate (%) (1) for MB and RB and the maximum amount of MB and RB adsorbed in equilibrium (qe) (2) are calculated by the following formulas.[15,28,35,37–39]

$$\text{RemovalRate}(\%) = c(C_0 - C_e)C_0x100 \quad (1)$$

Adsorption Capacity, q_e (mg/g)

$$= \frac{(C_0 - C_e)V}{W} \quad (2)$$

Where C_0 and C_e are defined as the initial and equilibrium concentrations of MB and RB (mg/L), V as the total volume of adsorbate solution (L), and W as the amount of adsorbent (g).[12,13]

For isotherm study, It was performed with 50 ml dye solutions at different temperatures (MB, RB; 293 K, 303 K, 313 K), and different concentrations (MB; 60–200 mg/L, RB; 20–50 mg/L) were determined under optimum conditions. Then, samples were shaken in a mixing device for 24 hours to examine the adsorption process, and then readings were done on a UV-Visible spectrophotometer.

Kinetic and isotherm modeling

Defining the adsorption kinetic performance and determining the reaction order is important to understand the adsorption mechanism and process. Kinetic performance is important for pilot applications.[3] Many kinetic models are used to explain adsorption kinetics..[12,40] In this study, pseudo-first-order, pseudo-second-order, and Elovich kinetic models were used to investigate the adsorption kinetics of MB and RB by CBM.

Adsorption isotherm studies get importance when it comes to the equilibrium of adsorption.[41] The nonlinear correlations between the concentration of adsorbate remaining in the solution (C_e) and the amount of substance retained per unit weight of the adsorbent (q_e) are defined as isotherms.[11] The Langmuir, Freundlich, and Temkin isotherm models, which are widely used in dye adsorption studies, have been determined in this

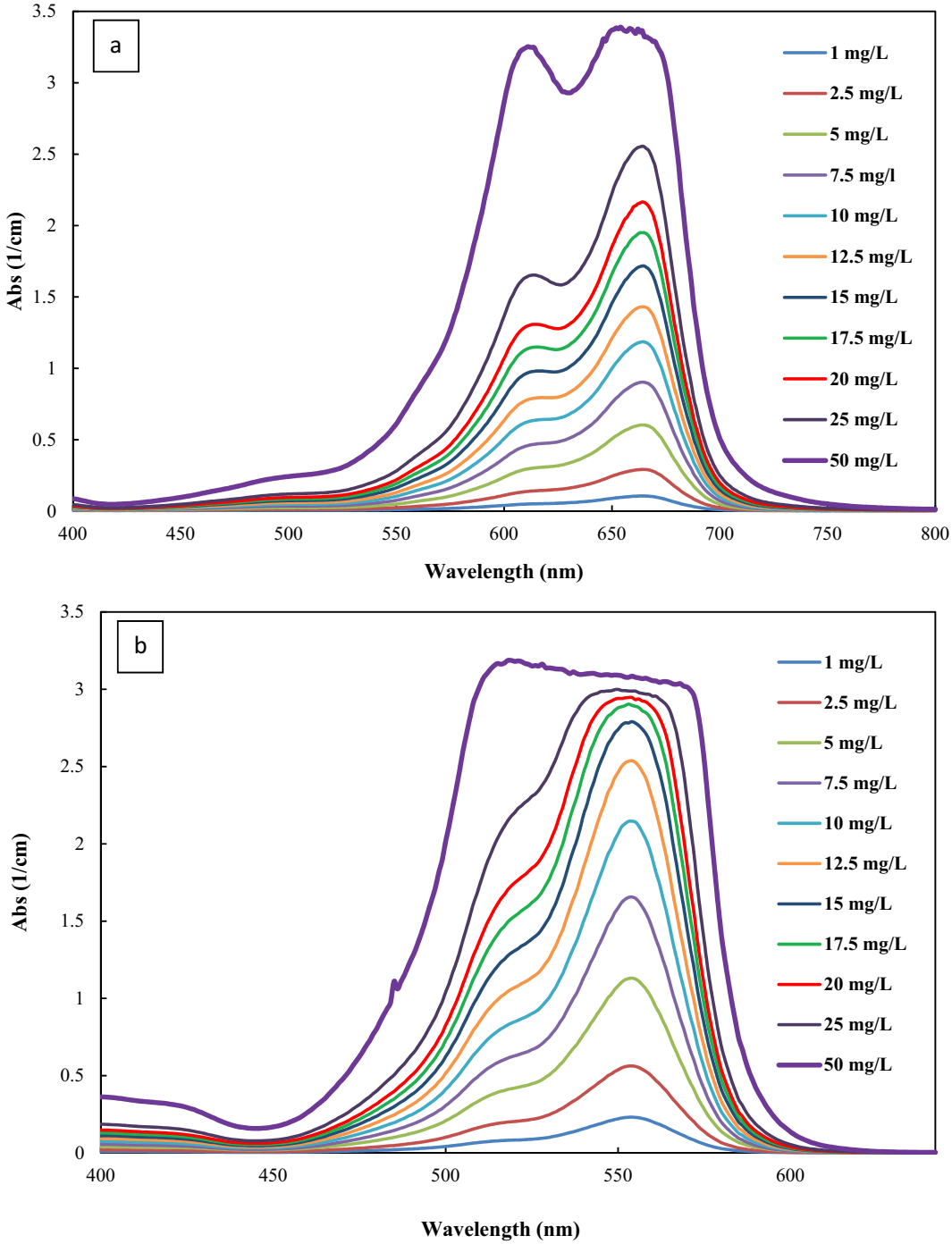

Figure 1. UV-VIS absorption spectra of 1–50 mg L^{-1} (a) Methylene Blue and (b) Rhodamine B.

study. The formulas and parameters used for the adsorption kinetics and isotherms used in this study are given in Table 1.

k_1 (min^{-1}): *Pseudo-first-order rate constant*
k_2 (g mg^{-1} min^{-1}): *Pseudo-second-order rate constant*
β (g mg^{-1}): *Elovich constant*
α (mg g^{-1} min^{-1}): *Initial adsorption rate*
q_e (mg/g): *Adsorption capacities (equilibrium)*
q_t (mg/g): *Adsorption capacities at time t*
q_m (mg/g): *Langmuir model maximum adsorption capacity*
K_L (L mg^{-1}): *Langmuir model adsorption constant*
K_F ((mg/g) $(L/mg)^{1/n}$): *Freundlich constant*
n: *Freundlich exponent*

Table 1. Adsorption equilibrium isotherm and kinetic models.

Models	Equations	Reference
Kinetic		
Pseudo-First-Order	$\log(q_e - q_t) = logq_e - \frac{k_1}{2.303}t$	[42]
Pseudo-Second-Order	$\frac{t}{q_t} = \frac{1}{q_e^2 k_2} + \frac{1}{q_e}t$	[43]
Elovich	$q_t = \frac{1}{\beta}\ln(\alpha\beta) + \frac{1}{\beta}lnt$	[44]
Isotherm		
Langmuir	$\frac{1}{q_e} = \frac{1}{q_m K_L}\frac{1}{C_e} + \frac{1}{q_m}$	[45]
Freundlich	$logq_e = logK_F + \frac{1}{n}logC_e$	[11]
Temkin	$q_e = \frac{RT}{B}lnC_e + \frac{RT}{B}lnA$	[46]

R (J/(mol K)): *Gas constant, 8.314 J/mol·K*

T (K): *Temperature*

B (J mol^{-1}): *Temkin constant related to the heat of adsorption*

A (L mg^{-1}): *Temkin constant*

Thermodynamics studies

The temperature-dependent change in adsorption thermodynamics is examined and thermodynamic studies are carried out to determine the nature (whether it occurs spontaneously or not) of the adsorption process at different temperatures.[47]Thermodynamic experiments of MB and RB adsorption on CBM were carried out at 293 K, 303 K and 313 K temperatures. Adsorption isotherm data were used to calculate the Gibbs free energy change (ΔG°), enthalpy (ΔH°) and entropy (ΔS°) parameters. Thermodynamic parameters are calculated by the following formulas (3–6).

$$\Delta G^{\circ} = -RTlnKd \tag{3}$$

$$K_d = \frac{qe}{Ce} \tag{4}$$

$$lnK_d = \frac{\Delta S^{\circ}}{R} - \frac{\Delta H^{\circ}}{RT} \tag{5}$$

$$\Delta G = \Delta H - T\Delta S \tag{6}$$

Where ΔG° Gibbs free energy change (kJ/mol), ΔH° enthalpy (kJ/mol), ΔS° entropy change (kJ/mol.K), R gas constant (J/(mol K)), T temperature (K), is the K_d distribution coefficient. Unknown constants were calculated from the slope and intercept of plots LnK_d versus 1/T.

Determination of pH zero charge point (pH_{pzc})

With the determination of pH_{pzc}, the pH values at which the adsorbent surface is neutral, positive and negative can be determined. When $pH_{pzc,adsorbent} < pH_{solution}$, the net surface charge of the adsorbent becomes negative and this shows that better results can be obtained for adsorbing solutions with cationic character. When $pH_{pzc,adsorbent} > pH_{solution}$, the net surface charge of the adsorbent material is positive and this means that better results can be obtained for adsorbing solutions with anionic character.

In this study, pH drift method was used for pH_{pzc} adsorbent.[48,49] 0.05 mol/L NaCl solution was prepared. 20 ml of NaCl solution in flasks was adjusted to different pH values in the range of 2–10 with 0.1 M HCl and NaOH. The total volume was made up to 30 ml with NaCl. Initial pH values were recorded. 50 mg of CBM was added to them and mixed at 25 °C for 48 hours. The final pH values of each solution were then measured. The graph in Fig. 2 was created with the obtained data. Accordingly, it is seen that the $pH_{pzc,CBM}$ value is 8.1.

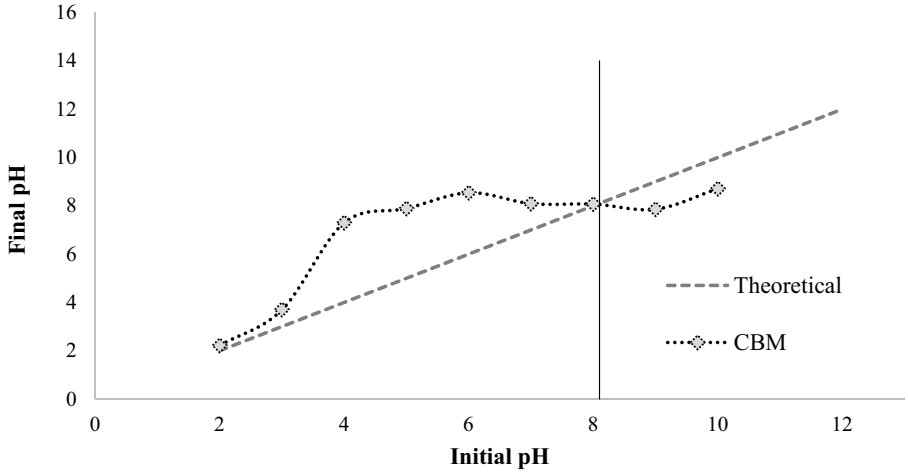

Figure 2. Determination of the point of zero charge of pH.

Regeneration

After the adsorbent reaches its saturation point, its regeneration is an important issue to minimize operating costs, reduce the disposal of the used adsorbent, and increase the reusability of the adsorbent.[22] After the adsorption experiments, CBM was collected for MB and RB under optimum conditions. The exhausted CBM was kept under UV light for 3 hours after air drying. After this process, adsorption experiments were carried out with regenerated CBM and the removal efficiencies were investigated.

Results and discussion

Properties of CBM

Novel recycled carbon-based material contains 46% fixed carbon, 41.9% volatile matter, 67.7% carbon, 6% hydrogen and 21.4% oxygen (Table 2). The surface area of carbon-based material produced from end-of-life tires is 35.5 m^2/g (Table 3).[29,30]

a, by weight difference; b is calculated with the Beckman formula. FC: Fixed Carbon, VM: Volatile Matter, H: Humidity, GHV: Gross Heating Value

According to the XRD spectrum of CBM (Fig. 3a), $CaCO_3$ and activating ZnO additives used in waste tire production were transformed into $Ca_{14}Si_{19}$, ZnS, $NaZn_{13}$ and SiC compounds as a result of chemical decomposition and it was determined that the CBM was in amorphous structure.

The most prominent peaks were found as 284.33 eV C-C peak (C1s), [50] 498.33 eV Zn-Na peak, [51] 532.33 eV O-Na (O1s), [52] 1073.33 eV Na peak (Na1s)[53] in the XPS spectrum of CBM.

In the elemental analysis results of CBM, it was determined that 67.7% carbon, amorphous (Fig. 3a), pure S2p structure (Fig. 3c) and 21.4% oxygen, metal oxide (Fig. 3c) and C-O (Fig. 3d) form. On the other hand, 6% hydrogen has formed a C-H bond in the CH_2 structure (Fig. 3d).

The use of new carbon-based material in dyestuff removal ensures the utilization of waste tires. Compared to the adsorbents used in the literature, it is one of the most important features that it removes very well when used in small amounts and is used repeatedly with regeneration.

Effect of operational parameters

Adsorbent dosage and contact time

Choosing an appropriate adsorbent dosage is essential for both resource savings and cost.[17,54] The effect of the adsorbent dosage was determined at room temperature, at 200 rpm agitation speed, and the original pH value for both dyes, holding constant 10 mg/L for the initial MB and RB concentration. Experiments were carried out in the range of 0.1–0.5 g/L for MB and 0.1–0.75 g/L for RB. The removal rate (%) and adsorption capacities (q_e) of MB and RB dyes in different adsorbent doses are presented in Fig. 4. When the removal rate against time is examined, it is seen that MB reaches the equilibrium in 60 minutes and RB in 120 minutes. The removal percentage increased from 70.0% to 97.1% when the adsorbent dose increased from 0.1 g/l to 0.5 g/L in 60 minutes for MB. However, the removal rate in 120 minutes for RB risen from 40.3% to 90.0% when the adsorbent dose increased from 0.1 g/l to 0.75 g/l. Commonly, the expansion in the active sites of the adsorbent surface area with a high dose increases the percentage of dye removal.[11,17,54]

When the adsorbent dose increased from 0.1 g/L to 0.5 g/L at 60 minutes for MB, the adsorption capacity also decreased from 72.8 mg/g to 22.3 g/L. When the adsorbent dose increased from 0.1 g/L to 0.75 g/L, the adsorption capacity decreased from 38.3 mg/g to 11.7 mg/g for RB at 120 minutes. The primary reason for this the increase in the adsorbent dose provides more surface area and active sites for MB and RB adsorption..[54] In addition, the increase in the mass of the adsorbent will decrease the adsorption capacity due

Table 2. Elemental analysis values of carbon-based material recovered from end-of-life tire[29].

	FC (%)	VM (%)	Ash (%)	H (%)	C (%)	H (%)	N (%)	O[a] (%)	S (%)	GHV[b] (Mj/kg)
CBM	46	41.9	6.91	5.21	67.7	6	0.065	21.4	4.87	27.8

Table 3. Surface area values of carbon-based material generated from end-of-life tire[29].

	S_{BET} (m^2/g)	Sext (m^2/g)	Smic (m^2/g)	Vt (cm^3/g)	Vmic (cm^3/g)	Vmezo (cm^3/g)	Avg. Pore Width (m^2/cm^3)	Pore Size (A°)
CBM	35.5	39.7	0	0.125	0	0.125	0.014	414

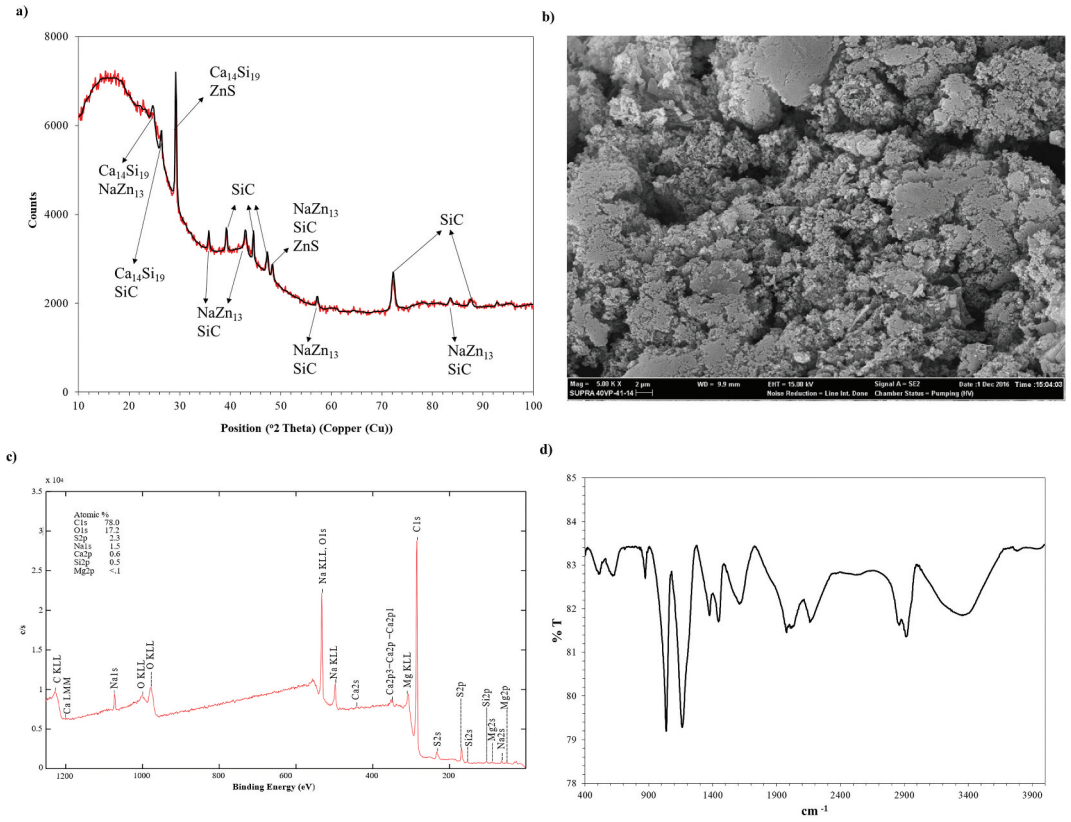

Figure 3. **a)** XRD **b)** SEM **c)** XPS **d)** FT-IR of CBM.

to the constant initial concentration and volume of MB and RB..[17,55] According to these analyzes, considering both the removal rate and the adsorption capacity, the optimum dose is 0.25 g/L for MB and 0.5 g/L for RB.

pH

Dyes pH is one of the most important factors affecting the sorption behavior in the adsorption process.[56] The pH can change the surface properties of the adsorbent material and the chemical structure of the dye solution.[54,57] Fig. 5 shows the relationship between solution pH and time-dependent MB and RB removal efficiency. MB's original pH value is 5.84 on average, and RB is 4.93. When the MB results are examined, it is seen that the increase or decrease in pH in the equilibrium time remains constant (about 95%) on the removal efficiency and does not have a significant effect on the MB solution. When the RB removal efficiencies were examined, there was a minimal increase (pH_9 = %80.7, pH_7 = %80.1, $pH_{original}$ = %86.5, pH_4 = %90.7, pH_9 = % 97.7) as the pH decreased. Therefore, the original pH values for both MB and RB solutions were selected as optimum for a cost-effective treatment without additional chemicals in the adsorption process.

Initial dye concentration

Figure 6 shows the relationship between removal rates at different initial dye concentrations. The results show that there are lower removals with increasing contact time and initial dye concentration. This is due to the saturation of the active sites on the surface of the adsorbent material. When it increased from 5 mg/L to 20 mg/L for MB, removal efficiency decreased from 97.0% to 93.8%. Similarly, when RB increased from 2.5 mg/L to 15 mg/L, a decrease was observed from 93.2% to 78.7%. In addition, the dye concentration may be related to the adsorption capacity of the adsorbent. While the adsorption capacity of 5 mg/L MB concentration was 23.5 mg/g, it increased to 80.3 mg/g at 20 mg/L MB concentration. While the adsorption capacity of 5 mg/L RB was 4.7 mg/g, it increased to 20.0 mg/g at 15 mg/L concentration.

Agitation speed

Agitation speed is another parameter directly related to the adsorption rate in the adsorption process. In this study, studies were carried out at 100, 150, and 200 rpm agitation speeds. The effect of agitation speed on dye adsorption efficiency is shown in Fig. 7. While approximately the same removal efficiencies were obtained at equilibrium time at 150 and 200 rpm for both dyes, very low removal

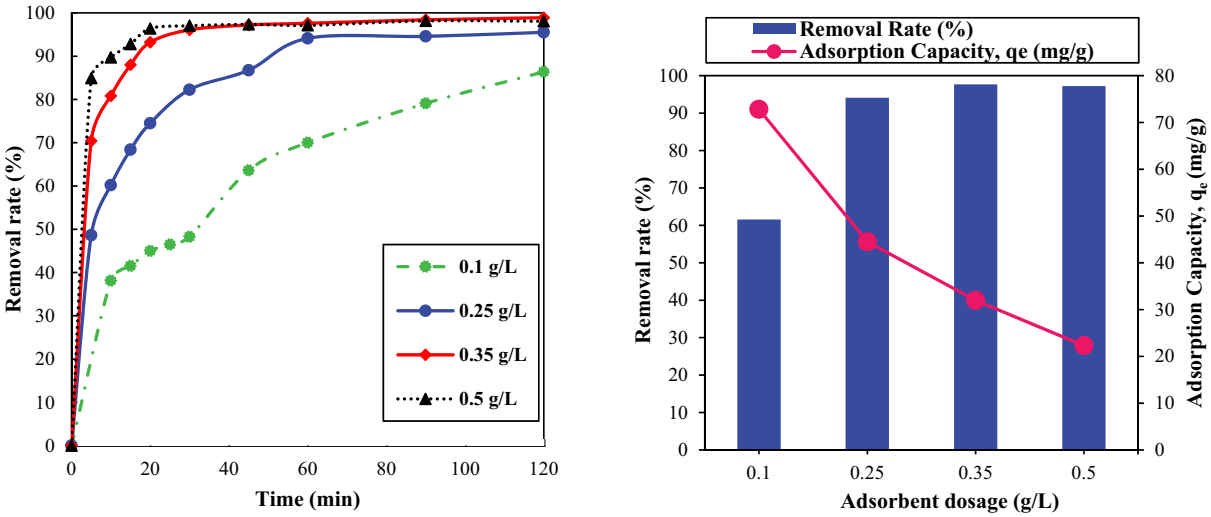

a) Methylene Blue

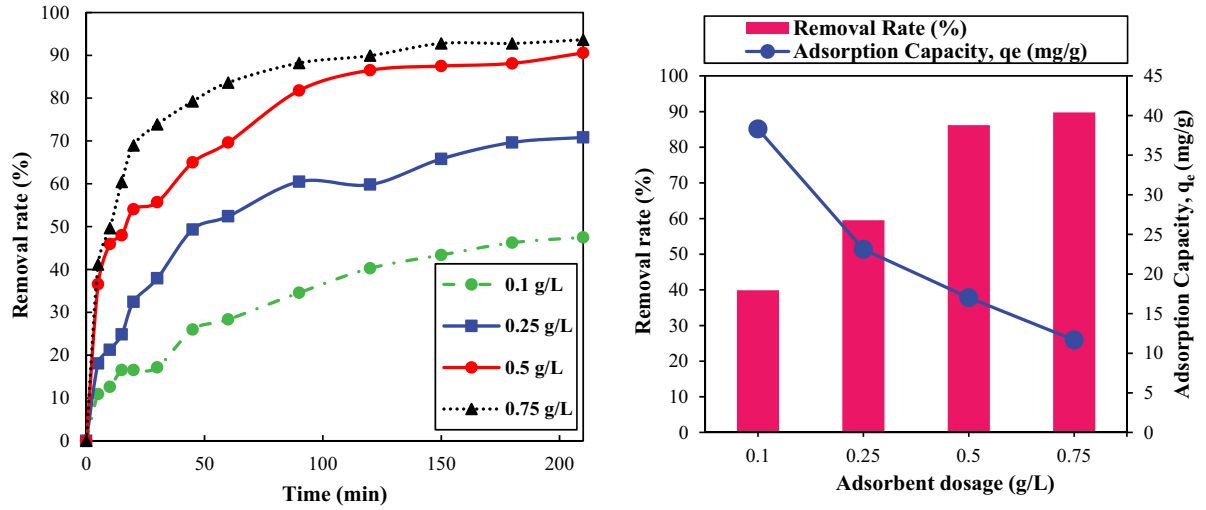

b) Rhodamine B

Figure 4. Removal rate and adsorption capacity of (a) MB and (b) RB at the effect of different adsorbent dosages (pH = Original, C_0 = 10 mg/L, 200 rpm, T = Room temperature).

efficiencies were obtained when the agitation speed was decreased (100 rpm). Therefore, it was concluded that 150 rpm agitation speed was appropriate in this study.

Temperature

Another critical parameter in the adsorption process is the temperature effect. Figure 8 shows the effect of MB and RB removal rate due to temperature change using CBM. When the results are examined, minimal changes are observed for both dyes in the removal efficiency at different temperatures. Nevertheless, considering these changes, the increase in the temperature shows that the increase in the removal efficiency, albeit slightly, shows that the adsorption is naturally endothermic. In all other experiments, the room temperature (293 K-300 K) was chosen as the operating temperature without any change to ensure high efficiency and energy savings.

Adsorption kinetics

Kinetic models have been developed to describe the kinetic process of adsorption and to determine the degree of reaction. In kinetic studies, adsorption

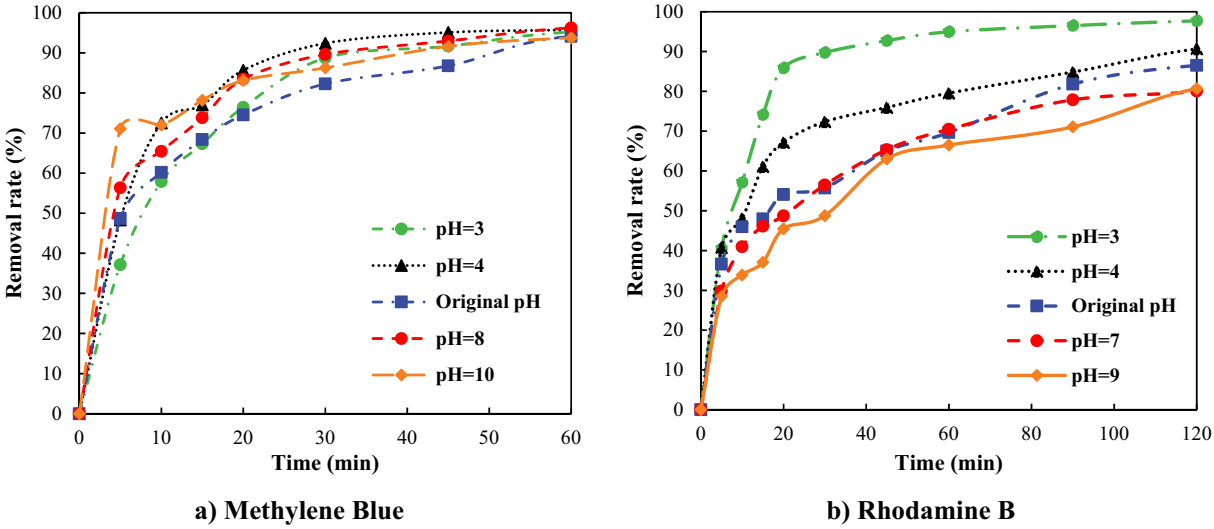

Figure 5. Effect of different pH (a) MB and (b) RB ($MB_{Adsorbent\ dose}$ = 0.25 g/L, $RB_{Adsorbent\ dose}$ = 0.5 g/L,C_0 = 10 mg/L, 200 rpm, T = Room temperature).

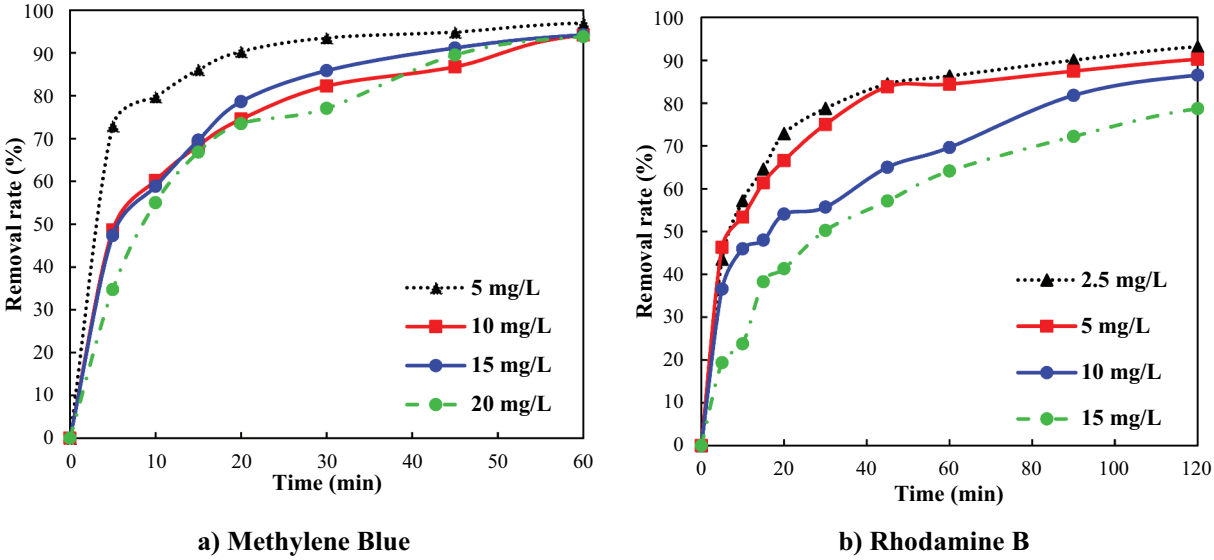

Figure 6. Effect of initial dye concentration (a) MB and (b) RB ($MB_{Adsorbent\ dose}$ = 0.25 g/L, $RB_{Adsorbent\ dose}$ = 0.5 g/L, pH = Original, 200 rpm, T = Room temperature).

capacity can be determined, and kinetic performance is of great importance for pilot applications. Adsorption kinetics are determined by fitting the adsorption capacities against time under optimum conditions. In this study, the adsorption of MB and RB dyes on CBM was investigated by pseudo-first-order, pseudo-second-order, and Elovich kinetic models. The kinetics of the experimental data have been obtained using the equations shown in Table 1. The parameters of the calculated kinetic models of the graphs (Supplementary Material 1) are explained in Table 4.

The results showed that the pseudo-second-order model for the adsorption of both RB and MB on CBM was most fitted with the significantly higher coefficient of correlation (R^2_{MB} = 0.9813, R^2_{RB} = 0.9975) when comparing the three models. In addition, as can be seen in Table 4, the fact that the value of $q_{e,\ experiment}$ (41.7 mg/g and 17.1 mg/g) is close to the theoretical value of qe (46.3 mg/g and 17.3 mg/g) calculated by the pseudo-second-order model that can also show its compatibility with this model. Compliance with this kinetic model also predicts that

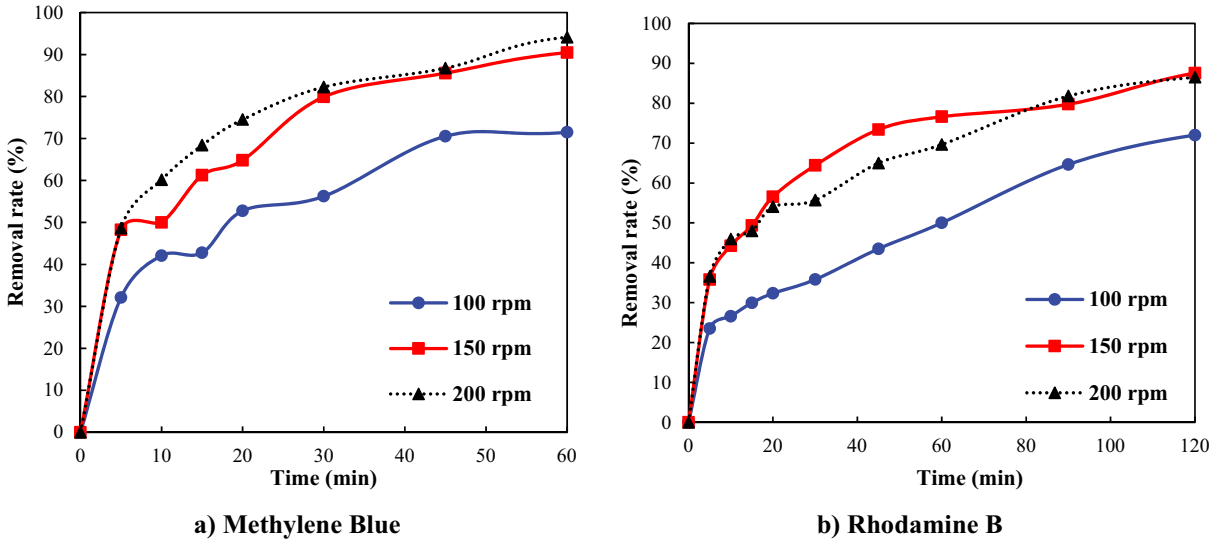

Figure 7. Effect of agitation speed (a) MB and (b) RB ($MB_{Adsorbent\ dose}$ = 0.25 g/L, $RB_{Adsorbent\ dose}$ = 0.5 g/L, pH = Original, C_0 = 10 mg/L, T = Room temperature).

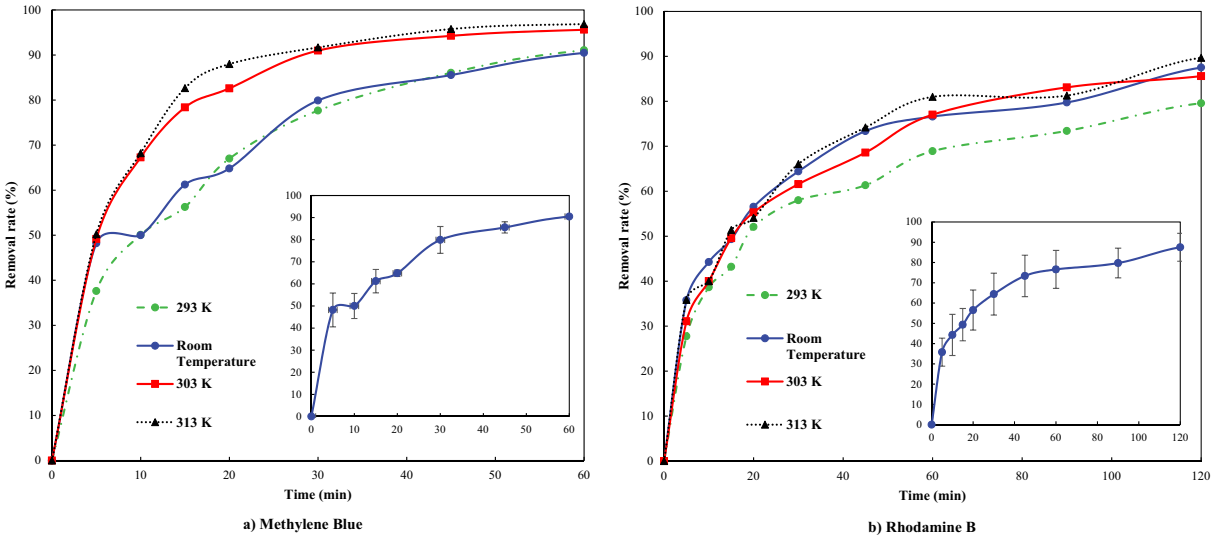

Figure 8. Effect of temperature (a) MB and (b) RB ($MB_{Adsorbent\ dose}$ = 0.5 g/L, $RB_{Adsorbent\ dose}$ = 0.25 g/L, pH = Original, C_0 = 10 mg/L, 150 rpm).

chemisorption (chemical adsorption) occurs until the adsorption of MB and RB by CBM reaches the equilibrium time.[17,54]

Adsorption isotherms

Langmuir, Freundlich, and Temkin isotherm models were used in this study to understand the adsorption properties. Adsorption isotherm experiments were performed at 0.25 g/L CBM for MB and 0.5 g/L CBM for RB, 50 ml MB (60–200 mg/L) and RB (20–50 mg/L)

Table 4. Kinetic models parameters for MB and RB adsorption on CBM.

		Dye	
Kinetic models	Model parameters	MB	RB
Pseudo-First-Order	$q_{e,\ experiment}$ (mg/g)	41.7	17.1
	q_e (mg/g)	30.8	9.93
	k_1, (min^{-1})	0.06	0.02
	R^2	0.9759	0.9532
Pseudo-Second-Order	q_e (mg/g)	46.3	17.3
	k_2 (g mg^{-1} min^{-1})	0.003	0,01
	R^2	0.9813	0.9975
Elovich	β (g mg^{-1})	0.12	0.31
	α (mg g^{-1} min^{-1})	17.1	5.02
	R^2	0.9165	0.9840

solutions at original pHs at different temperatures (293 K, 303 K, 313 K) and stirring at 150 rpm for 24 hours. The necessary calculations have been made using the isotherm equations given in Table 1 according to MB and RB concentrations before and after adsorption. The graphics obtained with the experimental results for the adsorption isotherm are shown in Fig. 9. Hence, it is seen that the maximum adsorption capacity ($q_{e,\ max}$) of the dye is 681 mg/g for MB and 85.3 mg/g for RB. Supplementary Material 2 shows the linear forms of the experimental data.

The model parameters obtained from these graphics are summarized in Table 5. Results show that the Freundlich isotherm is more fitting for explaining the adsorption process, with the highest R_{MB}^2 = 0.9971 (313 K) and R_{RB}^2 = 0.9970 (303 K) compared to Langmuir and Temkin isotherm.

The maximum adsorption capacity of MB and RB with CBM and other adsorbents is compared in Table 6. As a result of this comparison, it is seen that CBM has a higher potential for MB adsorption than most of the other adsorbent materials except for Hierarchical porous carbon. CBM adsorption capacity for RB is lower than MB adsorption. But, the maximum adsorption capacity for RB is quite good compared to other adsorbent amounts. In this sense, it can be concluded that CBM can be considered as an effective adsorbent in dye removal.

Adsorption thermodynamics

In accordance with the information given in section thermodynamics studies, the graphs obtained with the thermodynamic data are shown in Fig. 10. Thermodynamic parameters obtained with these graphs are given in Table 7.

According to Table 7, the Gibbs free energy change is negative ($\Delta G° < 0$) at all temperatures. Negative values indicate that the adsorption of MB and RB on the CBM occurs spontaneously. A positive enthalpy ($\Delta H° > 0$) means that the reaction is endothermic and a positive entropy ($\Delta S° > 0$) means that the reaction is irreversible.[62]

Regeneration

For the reusability of the CBM, the regeneration experiment was carried out as 6 cycles after the adsorption experiment, as explained in the 2.3.4 heading. The results obtained are given in Fig. 11.

As can be seen from Fig. 11, MB and RB removal performance of CBM gradually decreased with increasing adsorption cycles. While there was a 16% decrease for MB in the 4th cycle, a 26.5% decrease for the RB, at the end of the 6th cycle there was a 34.3% decrease for the MB and 48.7% for the RB. This is attributed to the partial recovery of active sites on the CBM after regeneration.[9] With this regeneration method used, it is seen that CBM has the potential to be a reusable adsorbent. However, the regeneration properties of CBM can be improved using other approaches and higher yields can be achieved.

CBM and dyes (MB and RB) interaction mechanism

FT-IR spectrum of CBM, MB adsorbed CBM (A-CBM_{MB}), and RB adsorbed CBM (A-CBM_{RB}) were given in Fig. 12 and Table 8 The peaks of CBM; 2930–2900 cm^{-1} C-H peak, 2160–1982 cm^{-1} C = O vibration stress, 1625 cm^{-1} C = C peak, 1446–1377 cm^{-1} C-H stretching, 1168 cm^{-1} C-O stretching, 1037 cm^{-1} C-O vibration peak, and 874 cm^{-1} C-H stretch.[63,64]

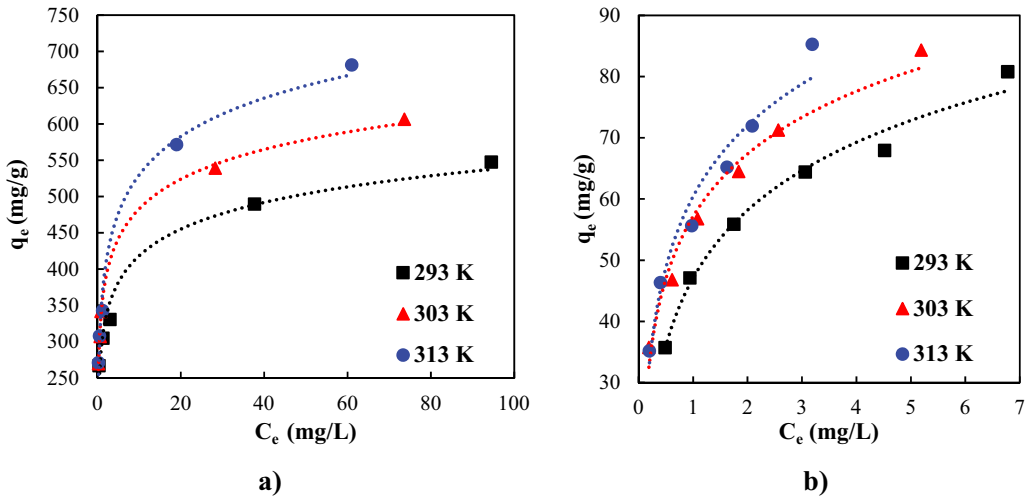

Figure 9. Effect of initial concentration on adsorption of (a) MB (b) RB adsorption onto CBM.

Table 5. Calculated parameter values isotherm models for the adsorption of MB and RB on CBM.

		Langmuir			Freundlich			Temkin		
Dyes	Temperature (K)	K_L (L mg^{-1})	q_m (mg/g)	R^2	K_F (mg/g)(L/mg)$^{1/n}$	n	R^2	A (L mg^{-1})	B (J mol^{-1})	R^2
MB	293	3.83	435	0.6881	295	7.11	0.9944	267	46.0	0.9815
	303	4.00	500	0.8050	335	7.11	0.9948	352	43.0	0.9968
	313	3.17	526	0.8208	339	5.83	0.9971	103	34.1	0.9893
RB	293	1.65	78.7	0.9793	45.9	3.43	0.9828	18.9	152	0.9831
	303	4.76	72.5	0.8954	55.0	3.79	0.9970	48.0	171	0.9777
	313	4.00	78.13	0.9492	58.0	3.32	0.9882	36.8	155	0.9598

Table 6. Comparison of maximum adsorption capacities ($q_{e,max}$) for MB and RB dyes on different adsorbents.

Adsorbent	Adsorbent Dose (g/L)	Max Adsorption Capacity, $q_{e,max}$ (mg/g)	Reference
Methylene Blue (MB)			
NaOH-biochar	1.4	105	[58]
Wet-torrefied microalgal biochar	1	113	[17]
Magnetic activated carbon (Fe-AC)	0.5	357	[59]
Hierarchical porous carbon	0.2	844	[57]
End-of-life tire-derived CBM	0.25	681	**This Study**
Rhodamine B (RB)			
Earthworm manure biochar	2	21.6	[60]
Cassava slag biochar	4	105	[54]
Activated sugar-based carbon	0.8	124	[11]
Biochar from plive biomass waste	0.7	264	[61]
End-of-life tire-derived CBM	0.5	85.3	**This Study**

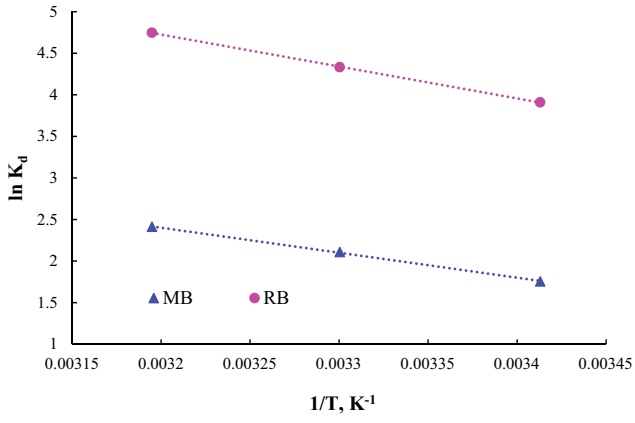

Figure 10. Effect of thermodynamics on adsorption of MB and RB on CBM at different temperatures.

Table 7. Thermodynamic parameters values for RB and MB onto CBM.

Dyes	T (K)	ΔH° (kJ/mol)	ΔS° (kJ/mol.K)	ΔG° (kJ/mol)
MB	293	25,02	0,10	−4,29
	303			−5,29
	313			−6,29
RB	293	31,92	0,14	−9,52
	303			−10,93
	313			−12,35

2160–1982 cm^{-1} C = O vibration stress and 1625 cm^{-1} C = C peak seen in CBM were not observed in A-CBM_{MB}. 3440 cm^{-1} N-H stretch, [63] ~614 cm^{-1} CH vibration, [65] and ~534 cm^{-1} phenyl ring planar ring deformation[66] were observed in A-CBM_{MB}. These peaks were not observed in CBM. This is proof that methylene blue is adsorbed on the CBM.

2160–1982 cm^{-1} C = O vibration stress and 874 cm^{-1} C-H stretch peak seen in CBM were not observed in A-CBM_{RB}. 3440 cm^{-1} N-H stretching[63] and planar ring deformation of ~534 cm^{-1} phenyl ring[66] were observed in A-CBM_{RB}. The fact that these peaks are not observed in the CBM is proof that Rhodamine B is adsorbed on the CBM.

According to the FT-IR results, both dyes were attached to the CBM surface from the same regions. The binding reactions of the dyes to the CBM surface are shown in Fig. 13.

SEM images of CBM, A-$CBM_{MB,}$ and A-CBM_{RB} were given in Fig. 14. It was observed that the adsorbent surface morphology changed significantly after the dyes were adsorbed on the CBM surface. A heterogeneous distribution was observed on the A-CBM_{MB} surface where MB was adsorbed. It was observed that there were larger particles and a more homogeneous distribution on the A-CBM_{RB} surface where Rhodamine B was adsorbed.

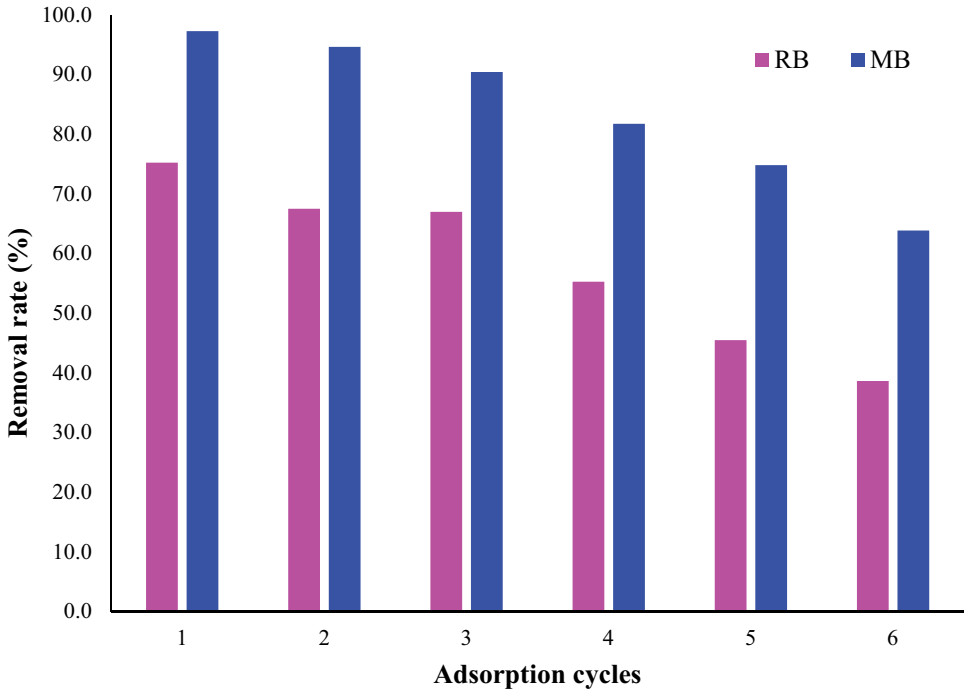

Figure 11. Removal rate (%) on the reused CBM.

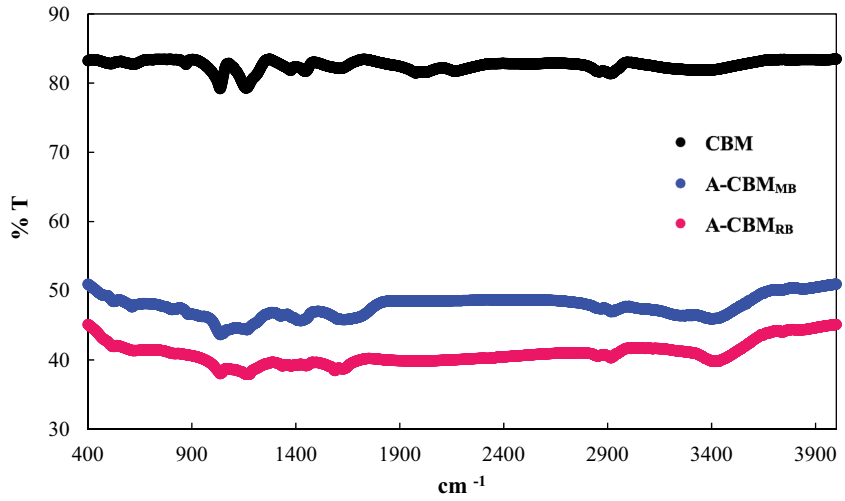

Figure 12. FT-IR spectrum of CBM, A-CBM_{MB}, and A-CBM_{RB}.

Table 8. FT-IR spectrum statements of CBM, A-CBM_{MB} and A-CBM_{RB}.

CBM (cm^{-1})	A-CBM_{MB} (cm^{-1})	A-CBM_{RB} (cm^{-1})	Comments
– –	3440	3440	N-H stretching[63]
2930–2900	2930–2865	2925–2860	C-H group in CH_2. Hydrogen bonds from an sp3-hybridized carbon[63,64]
2160–1982	– –	– –	C = O vibration stretching[64]
– –	~1680	– –	C = O vibration stretching[63]
1625	– –	1640–1590	C = C peak[63,64]
1446–1377	1433–1332	1454	C-H stretching[64]
1168	1171	1183	C-O stretching[63,64]
1037	1052	1048	C-O vibration peak[63,64]
874	809	– –	C-H stretching[63,64]
– –	~614	– –	C-H[65]
– –	~534	~528	Planar ring deformation of the phenyl ring[66]

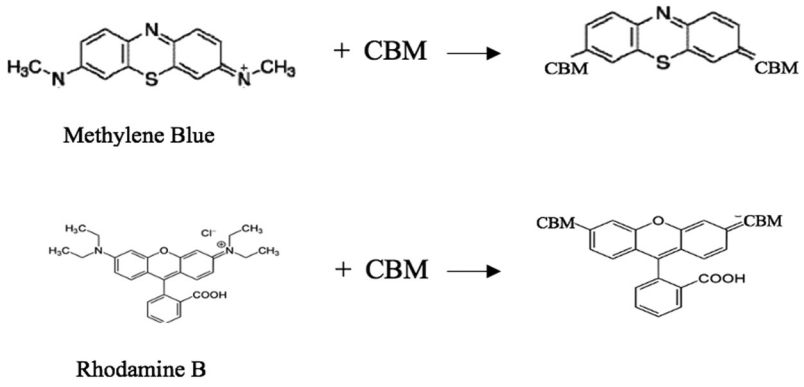

Figure 13. Reactions between CBM and dyes (MB and RB).

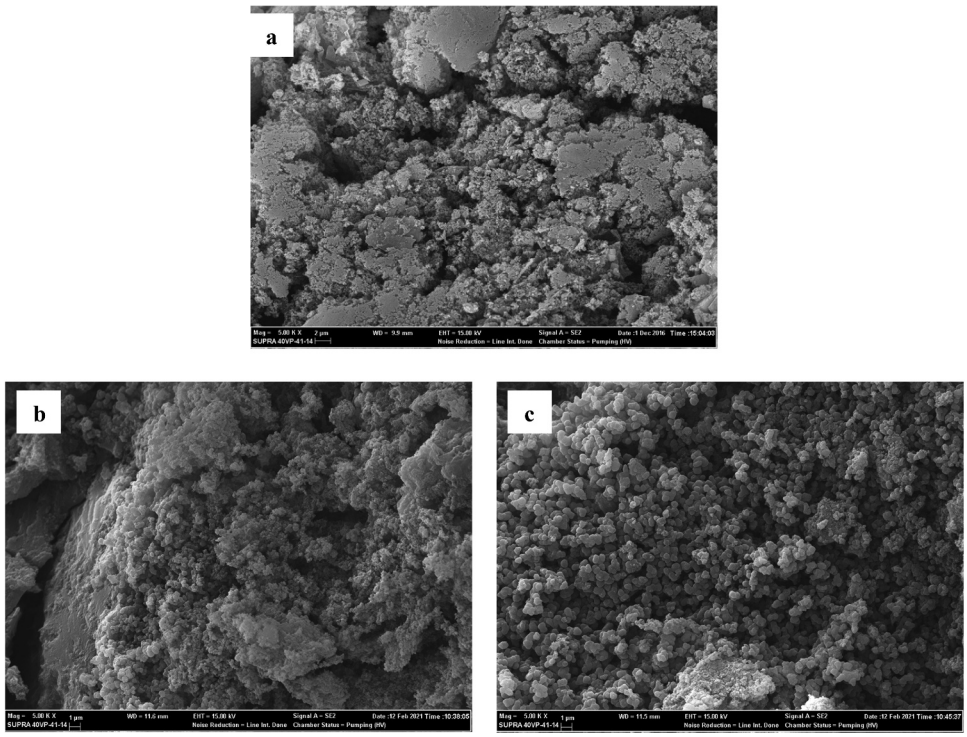

Figure 14. SEM images of (a) CBM, (b) A-CBM_{MB} and (c) A-CBM_{RB}.

Conclusion

A carbon-based material recycled from end-of-life tires (ELTs) using a novel patented process unlike the pyrolysis and carbonization methods in the literature is studied. CBM was used as an adsorbent in organic dyes removal. Experimental results have shown that MB and RB adsorption by CBM is fitted to the Freundlich isotherm. In addition, the MB and RB adsorption behavior fits to the pseudo second-order kinetic model. The maximum adsorption capacity of MB and RB on CBM is 681 and 85.3 mg/g, respectively. This high adsorption capacity means that CBM is a promising adsorbent that can be used for dye removal. The application of CBM produced from end-of-life tires in dye adsorption has shown that it is a good practice for recovering. Within the scope of end-of-life tires (ELTs) management, reuse of tires according to the circular economy model is becoming increasingly important.

These results indicate that CBM is a suitable candidate for effective adsorption dye removal of methylene blue, rhodamine B, and other dyes and also holds promise for use in other applications in water/wastewater treatment.

Highlights

- This carbon-based material (CBM) has been produced by novel patented method and used for the first time for organic dye removal in the literature.
- The novel CBM showed maximum adsorption capacity for methylene blue (MB) (681 mg/g) and Rhodamine B (85.3 mg/g).
- CBM can be used as a novel precursor adsorbent in dye-intensive industries such as the textile industry wastewater treatment.

Acknowledgements

This work was supported by the Eskisehir Technical University Scientific Research Projects Commission (Project Number: 20ADP123). One of the authors (ID) thanks TUBITAK 2211 scholarship program. The authors would also like to thank the anonymous reviewers and editors for commenting on this paper.

Data availability statement

The data that support the findings of this study are available from the corresponding author, [Z.Y.A.], upon reasonable request.

Disclosure statement

No potential conflict of interest was reported by the author(s).

ORCID

Zehra Yigit Avdan http://orcid.org/0000-0001-7445-3393

References

[1] Hasanpour, M.; Hatami, M. Photocatalytic Performance of Aerogels for Organic Dyes Removal from Wastewaters: Review Study. *J. Mol. Liq.* 2020, 309, 113094. DOI: 10.1016/j.molliq.2020.113094.

[2] Gupta, V. K.; Suhas. Application of Low-cost Adsorbents for Dye Removal – A Review. *J. Environ. Manage.* 2009, 90(8), 2313–2342. DOI: 10.1016/j.jenvman.2008.11.017.

[3] Natarajan, S.; Bajaj, H. C.; Tayade, R. J. Recent Advances Based on the Synergetic Effect of Adsorption for Removal of Dyes from Waste Water Using Photocatalytic Process. *J Environ Sci.* 2018, 65, 201–222. DOI: 10.1016/j.jes.2017.03.011.

[4] Bensalah, N.; Alfaro, M. A. Q.; Martínez-Huitle, C. A. Electrochemical Treatment of Synthetic Wastewaters Containing Alphazurine A Dye. *Chem. Eng. J.* 2009, 149(1), 348–352. DOI: 10.1016/j.cej.2008.11.031.

[5] Dawood, S.; Sen, T. K.; Phan, C. Synthesis and Characterisation of Novel-activated Carbon from Waste Biomass Pine Cone and Its Application in the Removal of Congo Red Dye from Aqueous Solution by Adsorption. *Water, Air, Soil Pollut.* 2014, 225(1), 1818. DOI: 10.1007/s11270-013-1818-4.

[6] Wróbel, D.; Boguta, A.; Ion, R. M. Mixtures of Synthetic Organic Dyes in a Photoelectrochemical Cell. *J. Photochem. Photobiol. A Chem.* 2001, 138(1), 7–22. DOI: 10.1016/S1010-6030(00)00377-4.

[7] Wu, C.-H. Adsorption of Reactive Dye onto Carbon Nanotubes: Equilibrium, Kinetics and Thermodynamics. *J. Hazard. Mater.* 2007, 144(1–2), 93–100. DOI: 10.1016/j.jhazmat.2006.09.083.

[8] Forgacs, E.; Cserháti, T.; Oros, G. Removal of Synthetic Dyes from Wastewaters: A Review. *Environ. Int.* 2004, 30(7), 953–971. DOI: 10.1016/j.envint.2004.02.001.

[9] Dai, L.; Zhu, W.; He, L.; Tan, F.; Zhu, N.; Zhou, Q.; He, M.; Hu, G. Calcium-rich Biochar from Crab Shell: An Unexpected Super Adsorbent for Dye Removal. *Bioresour. Technol.* 2018, 267, 510–516. DOI: 10.1016/j.biortech.2018.07.090.

[10] Alakhras, I.; Ouachtak, F.; Alhajri, H.; Rehman, E.; Al-Mazaideh, R.; Anastopoulos, G.; Lima, E. C. Adsorptive Removal of Cationic Rhodamine B Dye from Aqueous Solutions Using Chitosan-Derived Schiff Base. *Sep. Sci. Technol.* 57 4 2022, 542–554.

[11] Xiao, W.; Garba, Z. N.; Sun, S.; Lawan, I.; Wang, L.; Lin, M.; Yuan, Z. Preparation and Evaluation of an Effective Activated Carbon from White Sugar for the Adsorption of Rhodamine B Dye. *J. Cleaner Prod.* 2020, 253, 119989. DOI: 10.1016/j.jclepro.2020.119989.

[12] Wu, J.; Yang, J.; Feng, P.; Huang, G.; Xu, C.; Lin, B. High-efficiency Removal of Dyes from Wastewater by Fully Recycling Litchi Peel Biochar. *Chemosphere.* 2020, 246, 125734. DOI: 10.1016/j.chemosphere.2019.125734.

[13] Zhang, Y.; Su, P.; Weathersby, D.; Zhang, Q.; Zheng, J.; Fan, R.; Zhang, J.; Dai, Q. Synthesis of γ-Fe2O3-ZnO-biochar Nanocomposites for Rhodamine B Removal. *Appl. Surf. Sci.* 2020, 501, 144217. DOI: 10.1016/j.apsusc.2019.144217.

[14] Tan, K. B.; Vakili, M.; Horri, B. A.; Poh, P. E.; Abdullah, A. Z.; Salamatinia, B. Adsorption of Dyes by Nanomaterials: Recent Developments and Adsorption Mechanisms. *Sep. Purif. Technol.* 2015, 150, 229–242. DOI: 10.1016/j.seppur.2015.07.009.

[15] Rahimi Aqdam, S.; Otzen, D. E.; Mahmoodi, N. M.; Morshedi, D. Adsorption of Azo Dyes by a Novel Bio-nanocomposite Based on Whey Protein Nanofibrils and Nano-clay: Equilibrium Isotherm and Kinetic Modeling. *J. Colloid Interface Sci.* 2021, 602, 490–503. DOI: 10.1016/j.jcis.2021.05.174.

[16] Azhdarpoor, A.; Nikmanesh, R.; Khademi, F. A Study of Reactive Red 198 Adsorption on Iron Filings from Aqueous Solutions. *Environ. Technol.* 2014, 35(23), 2956–2960. DOI: 10.1080/09593330.2014.927007.

[17] Yu, K. L.; Lee, X. J.; Ong, H. C.; Chen, W.-H.; Chang, J.-S.; Lin, C.-S.; Show, P. L.; Ling, T. C. Adsorptive Removal of Cationic Methylene Blue and Anionic Congo Red Dyes Using Wet-torrefied Microalgal Biochar: Equilibrium, Kinetic and Mechanism Modeling. *Environ. Pollut.* 2021, 272, 115986. DOI: 10.1016/j.envpol.2020.115986.

[18] Arabiourrutia, M.; Lopez, G.; Artetxe, M.; Alvarez, J.; Bilbao, J.; Olazar, M. Waste Tyre Valorization by Catalytic Pyrolysis – A Review. *Renewable Sustainable Energy Rev.* 2020, 129, 109932. DOI: 10.1016/j.rser.2020.109932.

[19] Gupta, V. K.; Kumar, R.; Nayak, A.; Saleh, T. A.; Barakat, M. A. Adsorptive Removal of Dyes from Aqueous Solution onto Carbon Nanotubes: A Review. *Adv. Colloid Interface Sci.* 2013, 193-194, 24–34. DOI: 10.1016/j.cis.2013.03.003.

[20] Nguyet, P. N.; Hata, Y.; Maharjan, N.; Watari, T.; Hatamoto, M.; Yamaguchi, T. Adsorption of Colour from Dye Wastewater Effluent of a Down-flow Hanging Sponge Reactor on Purified Coconut Fibre. *Environ. Technol.* 2020, 41(10), 1337–1346. DOI: 10.1080/09593330.2018.1534000.

[21] Zhang, F.; Chen, X.; Wu, F.; Ji, Y. High Adsorption Capability and Selectivity of ZnO Nanoparticles for Dye Removal. *Colloids Surf. A.* 2016, 509, 474–483. DOI: 10.1016/j.colsurfa.2016.09.059.

[22] Santoso, E.; Ediati, R.; Kusumawati, Y.; Bahruji, H.; Sulistiono, D.; Prasetyoko, D. Review on Recent Advances of Carbon Based Adsorbent for Methylene Blue Removal from Waste Water. *Mater. Today Chem.* 2020, 16, 100233. DOI: 10.1016/j.mtchem.2019.100233.

[23] Saleh, T. A.; Al-Saadi, A. A.; Gupta, V. K. Carbonaceous Adsorbent Prepared from Waste Tires: Experimental and Computational Evaluations of Organic Dye Methyl Orange. *J. Mol. Liq.* 2014, 191, 85–91. DOI: 10.1016/j.molliq.2013.11.028.

[24] Ji, B.; Wang, J.; Song, H.; Chen, W. Removal of Methylene Blue from Aqueous Solutions Using Biochar Derived from a Fallen Leaf by Slow Pyrolysis: Behavior and Mechanism. *J. Environ. Chem. Eng.* 2019, 7(3), 103036. DOI: 10.1016/j.jece.2019.103036.

[25] Tian, X.; Zhuang, Q.; Han, S.; Li, S.; Liu, H.; Li, L.; Zhang, J.; Wang, C.; Bian, H. A Novel Approach of Reapplication of Carbon Black Recovered from Waste Tyre Pyrolysis to Rubber Composites. *J. Cleaner Prod.* 2021, 280, 124460. DOI: 10.1016/j.jclepro.2020.124460.

[26] Makrigianni, V.; Giannakas, A.; Deligiannakis, Y.; Konstantinou, I. Adsorption of Phenol and Methylene Blue from Aqueous Solutions by Pyrolytic Tire Char: Equilibrium and Kinetic Studies. *J. Environ. Chem. Eng.* 2015, 3(1), 574–582. DOI: 10.1016/j.jece.2015.01.006.

[27] Li, L.; Liu, S.; Zhu, T. Application of Activated Carbon Derived from Scrap Tires for Adsorption of Rhodamine B. *J Environ Sci.* 2010, 22(8), 1273–1280. DOI: 10.1016/S1001-0742(09)60250-3.

[28] Qi, -F.-F.; Ma, T.-Y.; Liu, Y.; Fan, Y.-M.; Li, J.-Q.; Yu, Y.; Chu, L.-L. 3D Superhydrophilic Polypyrrole Nanofiber Mat for Highly Efficient Adsorption of Anionic Azo Dyes. *Microchem. J.* 2020, 159, 105389. DOI: 10.1016/j.microc.2020.105389.

[29] Balbay, S.;. Chemical Decomposition of Waste Tires and Evaluation of the Obtained Products. In *Graduate School of Sciences Department of Chemical Engineering* PhD Dissertation ; Bilecik: Bilecik Seyh Edebali University, 2017.

[30] Balbay, S.; Acıkgöz, C. Devulcanization of Waste Tires by a Cheap and Economical Method and Evaluation of Them as Raw Materials Patent No: 2015/13034 . 2019.

[31] Balbay, S. Effects of Recycled Carbon-based Materials on Tyre. *J. Mater. Cycles Waste Manage.* 2020, 22(6), 1768–1779. DOI: 10.1007/s10163-020-01064-9.

[32] Balbay, A.; Yılmaz, Y.; Balbay, Ş 2021 . Characterization of E-glass/epoxy Modified with Recycled Rubber Particles and Multi-walled Carbon Nanotubes. *The European Journal of Science and Technology*. 23, 837–843.

[33] Açıkgöz, Ç.; Balbay, Ş.; İsmail, D 2021 . Isı Enerjisi Depolayan Faz Değişim Malzemelerinin Üretimi. *Bilecik Şeyh Edebali University Journal of Science*. 8(1), 173–185.

[34] Zhang, Y.; Cheng, Q.; Wang, D.; Xia, D.; Zheng, X.; Li, Z.; Hwang, J.-Y. Preparation of Pyrolytic Carbon from Waste Tires for Methylene Blue Adsorption. *Jom*. 2019, 71(10), 3658–3666. DOI: 10.1007/s11837-019-03658-7.

[35] Hou, Y.; Huang, G.; Li, J.; Yang, Q.; Huang, S.; Cai, J. Hydrothermal Conversion of Bamboo Shoot Shell to Biochar: Preliminary Studies of Adsorption Equilibrium and Kinetics for Rhodamine B Removal. *J. Anal. Appl. Pyrolysis*. 2019, 143, 104694. DOI: 10.1016/j.jaap.2019.104694.

[36] Tariq, M.; Muhammad, M.; Khan, J.; Raziq, A.; Uddin, M. K.; Niaz, A.; Ahmed, S. S.; Rahim, A. Removal of Rhodamine B Dye from Aqueous Solutions Using photo-Fenton Processes and Novel Ni-Cu@ MWCNTs Photocatalyst. *J. Mol. Liq.* 2020, 312, 113399. DOI: 10.1016/j.molliq.2020.113399.

[37] Fan, S.; Wang, Y.; Wang, Z.; Tang, J.; Tang, J.; Li, X. Removal of Methylene Blue from Aqueous Solution by Sewage Sludge-derived Biochar: Adsorption Kinetics, Equilibrium, Thermodynamics and Mechanism. *J. Environ. Chem. Eng.* 2017, 5(1), 601–611. DOI: 10.1016/j.jece.2016.12.019.

[38] Ouachtak, H.; El Haouti, R.; El Guerdaoui, A.; Haounati, R.; Amaterz, E.; Addi, A. A.; Akbal, F.; Taha, M. L. Experimental and Molecular Dynamics Simulation Study on the Adsorption of Rhodamine B Dye on Magnetic Montmorillonite Composite γ-Fe2O3@ Mt. *J. Mol. Liq.* 2020, 309, 113142. DOI: 10.1016/j.molliq.2020.113142.

[39] Khan, T. A.; Rahman, R.; Khan, E. A. Adsorption of Malachite Green and Methyl Orange onto Waste Tyre Activated Carbon Using Batch and Fixed-bed Techniques: Isotherm and Kinetics Modeling. *Model. Earth Syst. Environment.* 2017, 3(1), 38. DOI: 10.1007/s40808-017-0284-1.

[40] Guo, X.; Wang, J. A General Kinetic Model for Adsorption: Theoretical Analysis and Modeling. *J. Mol. Liq.* 2019, 288, 111100. DOI: 10.1016/j.molliq.2019.111100.

[41] Li, W.; Xie, Z.; Xue, S.; Ye, H.; Liu, M.; Shi, W.; Liu, Y. Studies on the Adsorption of Dyes, Methylene Blue, Safranin T, and Malachite Green onto Polystyrene Foam. *Sep. Purif. Technol.* 2021, 276, 119435. DOI: 10.1016/j.seppur.2021.119435.

[42] Yuh-Shan, H. Citation Review of Lagergren Kinetic Rate Equation on Adsorption Reactions. *Scientometrics*. 2004, 59(1), 171–177. DOI: 10.1023/B:SCIE.0000013305.99473.cf.

[43] Xiao, Y.; Azaiez, J.; Hill, J. M. Erroneous Application of Pseudo-second-order Adsorption Kinetics Model: Ignored Assumptions and Spurious Correlations. *Ind. Eng. Chem. Res.* 2018, 57(7), 2705–2709. DOI: 10.1021/acs.iecr.7b04724.

[44] Varank, G.; Demir, A.; Yetilmezsoy, K.; Top, S.; Sekman, E.; Bilgili, M. S. Removal of 4-nitrophenol from Aqueous Solution by Natural Low-cost Adsorbents *Indian Journal of Chemical Technology* 19 7–25 . 2012.

[45] Singh, N.; Nagpal, G.; Agrawal, S. Water Purification by Using Adsorbents: A Review. *Environ. Technol. Innovation*. 2018, 11, 187–240.

[46] Djelloula, C.; Hasseineb, A.; Hamdaouic, O. Adsorption of Cationic Dye from Aqueous Solution by Milk Thistle Seeds: Isotherm, Kinetic and Thermodynamic Studies. *Desalin. Water Treat.* 2017, 78, 313–320. DOI: 10.5004/dwt.2017.20920.

[47] Sharma, S.; Sharma, G.; Kumar, A.; AlGarni, T. S.; Naushad, M.; Alothman, Z. A.; Stadler, F. J. Adsorption of Cationic Dyes onto Carrageenan and Itaconic Acid-based Superabsorbent Hydrogel: Synthesis, Characterization and Isotherm Analysis. *J. Hazard. Mater.* 2022, 421, 126729. DOI: 10.1016/j.jhazmat.2021.126729.

[48] El Haddad, M.; Mamouni, R.; Saffaj, N.; Lazar, S. Removal of a Cationic Dye – Basic Red 12 – From Aqueous Solution by Adsorption onto Animal Bone Meal. *J. Assoc. Arab Univ. Basic App. Sci.* 2012, 12(1), 48–54. DOI: 10.1016/j.jaubas.2012.04.003.

[49] Calvete, T.; Lima, E. C.; Cardoso, N. F.; Dias, S. L. P.; Pavan, F. A. Application of Carbon Adsorbents Prepared from the Brazilian Pine-fruit-shell for the Removal of Procion Red MX 3B from Aqueous solution—Kinetic, Equilibrium, and Thermodynamic Studies. *Chem. Eng. J.* 2009, 155(3), 627–636. DOI: 10.1016/j.cej.2009.08.019.

[50] Morgan, D. J. Comments on the XPS Analysis of Carbon Materials. *C.* 2021, 7(3), 51.

[51] Posıtıons Of Photoelectron And Auger Lınes On The Bındıng Energy Scale (Al X-Rays). In Vol. 2021.

[52] Jhang, J.-H.; Boscoboinik, J. A.; Altman, E. I. Ambient Pressure X-ray Photoelectron Spectroscopy Study of Water Formation and Adsorption under Two-dimensional Silica and Aluminosilicate Layers on Pd (111). *J. Chem. Phys.* 2020, 152(8), 084705. DOI: 10.1063/1.5142621.

[53] Chastain, J.; King, R. C., Jr. *Handbook of X-ray Photoelectron Spectroscopy*; Perkin-Elmer: USA, 1992; pp 261.

[54] Wu, J.; Yang, J.; Huang, G.; Xu, C.; Lin, B. Hydrothermal Carbonization Synthesis of Cassava Slag Biochar with Excellent Adsorption Performance for Rhodamine B. *J. Cleaner Prod.* 2020, 251, 119717. DOI: 10.1016/j.jclepro.2019.119717.

[55] Wang, X.; Jiang, C.; Hou, B.; Wang, Y.; Hao, C.; Wu, J. Carbon Composite Lignin-based Adsorbents for the Adsorption of Dyes. *Chemosphere*. 2018, 206, 587–596. DOI: 10.1016/j.chemosphere.2018.04.183.

[56] Zhou, Y.; Lu, J.; Zhou, Y.; Liu, Y. Recent Advances for Dyes Removal Using Novel Adsorbents: A Review. *Environ. Pollut.* 2019, 252, 352–365. DOI: 10.1016/j.envpol.2019.05.072.

[57] Zhang, Y.; Ji, G.; Li, C.; Wang, X.; Li, A. Templating Synthesis of Hierarchical Porous Carbon from Heavy Residue of Tire Pyrolysis Oil for Methylene Blue Removal. *Chem. Eng. J.* 2020, 390, 124398. DOI: 10.1016/j.cej.2020.124398.

[58] Mu, Y.; Ma, H. NaOH-modified Mesoporous Biochar Derived from Tea Residue for Methylene Blue and Orange II Removal. *Chemical Engineering Research and Design*. 2021, 167, 129–140. DOI: 10.1016/j.cherd.2021.01.008.

[59] Altıntıg, E.; Altundag, H.; Tuzen, M.; Sarı, A. Effective Removal of Methylene Blue from Aqueous Solutions Using Magnetic Loaded Activated Carbon as Novel Adsorbent. *Chemical Engineering Research and Design*. 2017, 122, 151–163. DOI: 10.1016/j.cherd.2017.03.035.

[60] Wang, Z.; Shen, D.; Shen, F.; Wu, C.; Gu, S. Kinetics, Equilibrium and Thermodynamics Studies on Biosorption of Rhodamine B from Aqueous Solution by Earthworm Manure Derived Biochar. *Int. Biodeterior. Biodegrad.* 2017, 120, 104–114. DOI: 10.1016/j.ibiod.2017.01.026.

[61] Albanio, I. I.; Muraro, P. C. L.; Da Silva, W. L. Rhodamine B Dye Adsorption onto Biochar from Olive Biomass Waste. *Water, Air, Soil Pollut.* 2021, 232(5), 1–11. DOI: 10.1007/s11270-021-05110-6.

[62] Tang, D.; Zheng, Z.; Lin, K.; Luan, J.; Zhang, J. Adsorption of P-nitrophenol from Aqueous Solutions onto Activated Carbon Fiber. *J. Hazard. Mater.* 2007, 143(1), 49–56. DOI: 10.1016/j.jhazmat.2006.08.066.

[63] Sigma-Aldrich, IR Spectrum Table & Chart. In.

[64] Ţucureanu, V.; Matei, A.; Avram, A. M. FTIR Spectroscopy for Carbon Family Study. *Crit. Rev. Anal. Chem.* 2016, 46(6), 502–520. DOI: 10.1080/10408347.2016.1157013.

[65] Rao, G.-S.; Nabipour, H.; Zhang, P.; Wang, X.; Xing, W.; Song, L.; Hu, Y. Lightweight, Hydrophobic and Recyclable Carbon Foam Derived from Lignin–resorcinol–glyoxal Resin for Oil and Solvent Spill Capture. *J. Mater. Res. Technol.* 2020, 9(3), 4655–4664. DOI: 10.1016/j.jmrt.2020.02.092.

[66] Trivedi, M. K.; Patil, S.; Shettigar, H.; Bairwa, K.; Jana, S. Effect of Biofield Treatment on Spectral Properties of Paracetamol and Piroxicam. *Chemical Sciences Journal*. 2015, 6(3 1–6).